Fuel 365 (2024) 131265

Contents lists available at ScienceDirect

Fuel

journal homepage: www.elsevier.com/locate/fuel

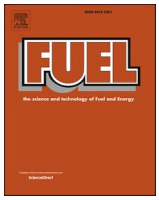

On the oxy-combustion of blends of coal and agro-waste biomass under dry and wet conditions

Luis I. Díez *, Alexander García-Mariaca, Eva Llera-Sastresa, Paula Canalís

Department of Mechanical Engineering, University of Zaragoza, María de Luna s/n, 50018 Zaragoza, Spain

ARTICLE INFO

Keywords:
Bio-CCS
Steam-moderated combustion
Agro-waste biomass
Burnout optimization
H_2O–NO interaction

ABSTRACT

Integrating bioenergy into carbon capture and storage systems (Bio-CCS) is a novel concept aiming at reducing CO_2 emissions, pointing to a short-term need to increase the use of non-conventional biomasses. The main objective of this experimental research is to characterize the behavior of two agro-waste biomasses under oxy-co-firing conditions, as concerns fuel conversion and NO formation, compared to the use of typical raw pine wood. The effect of replacing CO_2 with H_2O in the firing atmosphere is also sought. Two different biomass shares in the blends, 20 % and 50 %, are selected. The experiments are conducted in a lab-scale entrained flow reactor for two O_2 concentrations (21 % and 35 %) and four H_2O concentrations (0 %, 10 %, 25 %, 40 %). Some operating conditions are kept the same to enable the comparisons: mean residence time (3 s), initial reactor temperature (1000 °C) and oxygen excess (1.25). New results have been obtained from the experiments, optimizing burnout degrees and reducing NO levels. Minimum differences in conversions are detected for the 35 % O_2 cases when the agro-biomasses replace the pine wood: less than 0.7 and 1.1 percentage points. Burnout degrees are maximized when 25 % CO_2 is replaced with H_2O in most cases, with maximum values in the range 97.3–97.7 %. The higher the agro-biomasses share in the blend, the higher the N-fuel to NO conversion, consistent with their larger nitrogen contents. Significant decreases of NO are detected when CO_2 is replaced with H_2O, with maximum reductions of 17.6 %. The extent of these NO reductions shows a clear dependence on the volatiles-to-char ratios for the fired blends: the higher the ratio, the lower the decrease. For the largest steam additions (40 %), the NO depleting effect caused by H_2O is partially compensated with the enhancement of the N-volatiles oxidation, limiting the NO reductions to 1.7–7.3 % compared to the dry atmospheres.

1. Introduction

Global warming is a major concern that requires drastically curbing the increase in greenhouse gas emissions of anthropogenic origin. One of the main strategies relies on the decarbonization of power, chemical and energy-intensive industries. A wide set of research lines are now under development, aiming at increasing industrial energy efficiency [1,2], searching for alternative fuels [3,4], improving wastewater treatment technologies [5], decreasing the use of chemical fertilizers [6] or producing new soil amendments [7]. A promising avenue is to gradually reduce the reliance on fossil fuels, particularly coal, unlocking the potential of negative emissions technologies by integrating a carbon-neutral biofuel in capture and storage systems. In the pursuit of decarbonization, oxy-fuel combustion is one of the most suitable capture technologies [8]. For this reason, significant research has been mainly dedicated to the oxy-fuel combustion of pulverized coal [9], focused on addressing potential drawbacks and limitations [10].

While the positive impact of oxy-enriched atmospheres and biomass on reducing CO_2 emissions is acknowledged [11], oxy-co-combustion with non-conventional biomasses still deserves attention. So far, oxy-fuel experiences have encompassed from small-scale lab experiments like thermogravimetric analysis [12–14], drop tube furnaces [15,16] and entrained flow reactors [17–19], to large-scale facilities [20,21]. Regardless of size, efforts aim to improve efficiency, including fuel conversion and pollutant control.

In particular, NO_x formation during coal oxy-combustion has been investigated compared to conventional air-combustion, as well as the effect of replacing coal with biomass [22–24]. Usually, nitrogen content in biomass is lower than nitrogen in coal, which results beneficial to reduce NO_x formation. Oxy-fuel tests with sub-bituminous coal and sawdust showed that biomass particle size affected NO_x formation in air-fired conditions but not in oxy-fired conditions [25]. For coal + straw blends [26], increased oxygen in the primary airflow reduced HCN

* Corresponding author.
E-mail address: luisig@unizar.es (L.I. Díez).

https://doi.org/10.1016/j.fuel.2024.131265
Received 7 November 2023; Received in revised form 16 January 2024; Accepted 20 February 2024
Available online 26 February 2024

Nomenclature

A	Agro-biomass blend (corn + vineyard)
BET	Brunauer-Emmett-Teller
B	Biomass
C	Coal
c_p	Specific heat capacity (kJ/kmol K)
d	Particle diameter (μm)
$\dot{m}$	Mass flow rate (kg/s)
P	Pine wood
V	Vineyard pruning residues
α	Ash weight fraction, dry basis (–)
β	Burnout degree (%)
λ	Available oxygen/stoichiometric oxygen (–)
ρ	Density (kg/m^3)

formation and N_2O emissions due to higher furnace temperature. A larger share of straw in the blend increased both NO and N_2O emissions. In another study with rice husks, increasing the biomass ratio led to higher CO and CH_4 emissions but lower NO and NO_x emissions [27]. Tests with cornstalk and semi-coke showed better performance for blended fuel, with higher cornstalk ratios reducing CO, NO and N_2O emissions [28].

Compared to coal, the higher volatile content in biomass enhances NO formation due to the oxidation of the N-based precursors in the gas-phase, being NH_3 rather than HCN the predominant one [29]. Besides the nitrogen content in the fuel, the different oxidation kinetics of the N-volatiles and the N-char can significantly affect the rates of NO formation when coal is replaced with biomass [26,30,31]. Moreover, the alkali content in the mineral matter is reported to catalyst the NO − char depletion mechanism, according to the following steps [28,32]: 1) alkali metal ions in the char react with NO, resulting in metal oxide and a nitrogen radical; 2) metal oxides are reduced into alkali metal ions by reaction with carbon in the char, releasing carbon monoxide; 3) nitrogen radicals are combined to form N_2.

Recently, oxy-steam combustion has been suggested as a new technology that replaces CO_2 by condensed steam, which is re-evaporated before injection into the boiler. Steam serves to dilute oxygen and moderate flame temperature, eliminating the need for flue gas recycling [33,34]. The replacement of CO_2 by H_2O influences the conversion rates of coal and biomass due to a combination of factors: 1) the rise of the gas-phase temperature due to the lower molar specific heat of steam [35,36], 2) the increase of the oxygen diffusivity in the O_2/H_2O atmosphere surrounding the particles [37,38], 3) the intensification of char gasification rates caused by H_2O [39].

Gil et al. used thermogravimetric analysis to investigate the impact of steam on coal and biomass oxy-combustion [40]. Replacing up to 40 % of CO_2 with H_2O increased the mass-loss rate, reactivity, and shortened combustion time. Lei et al. conducted combustion tests with sewage sludge + pine sawdust and sewage sludge + bituminous coal particles in various atmospheres, finding that H_2O (up to 30 %) raised combustion temperature and shortened burnout time [41]. Rabaçal et al. studied particle fragmentation during the initial stages of conventional and dry/wet oxy-combustion with up to 10 % H_2O, observing an increase in fragmentation with H_2O [42].

Limited research has explored so far the NO emissions from biomass conversion in an oxy-steam environment. Moron et al. investigated NO_x emissions for coals, biomasses, and blends in air and dry/wet recirculated oxy-combustion atmospheres (up to 10 % H_2O). They observed a decrease in NO emissions when H_2O was added, indicating the role of CO in NO-to-N_2 reduction pathways [43]. Lu et al. found that H_2O addition (up to 15 %) resulted in NO reductions for four biomasses in an oxy-combustion environment [44]. Experimental results from oxy-co-firing tests of coal + biomass blends in a pulverized fuel burner showed increased NO_x emissions when H_2O in the recycled gases was removed [45].

Oxy-combustion could offer a good chance for low-to-mid-grade biomasses, with a very restricted use so far in conventional combustion. New knowledge and expertise in applying oxygen-enriched combustion to biomass under dry-recycle and wet-recycle conditions is crucial for advancing this field and even further towards oxy-steam combustion. The present work aims to provide novel experimental results encompassing three different types of biomass and various dry and wet oxy-combustion conditions. Results concerning burnout (solid-to-gas conversion), C-fuel conversion to CO and N-fuel conversion to NO are presented and discussed in the section 3.

2. Experiments

2.1. Fuels

Three domestic biomasses of different sources were selected to proceed with the experiments: 1) forest residues from pine wood, 2) agricultural residues from a mixture of 70 % woody vineyard and 30 % corn herbaceous wastes, 3) raw agricultural wastes from vineyard pruning. The two former were available in the form of pellets, and the third was in the form of chips. Table 1 summarizes the proximate and ultimate analysis of the biomass samples. Pine wood has low ash, nitrogen and chlorine contents. On the other hand, ash contents in the agro-biomasses are significantly higher: 7.3 % and 16.1 %, respectively. The very different levels of ash content in the biomasses were one of the selection criteria for these fuels, to detect their influence on the fuel conversion

Table 1
Proximate and ultimate analysis of the fuels.

	Bituminous coal **(C)**	Raw vineyard pruning **(V)**	Agro-biomass blend, corn + vineyard **(A)**	Pine wood **(P)**
Proximate analysis (% wt.)				
Moisture [1,5]	3.6	9.0	8.3	7.5
Volatile matter [2, 6]	25.9	64.0	69.4	76.8
Fixed carbon [10]	57.4	10.9	15.0	15.5
Ash [3, 7]	13.1	16.1	7.3	0.2
Volatiles-to-char ratio	0.36	2.37	3.11	4.89
Ultimate analysis (% wt., dry basis)				
Carbon [4, 8]	71.1	47.4	48.3	50.9
Hydrogen [4, 8]	3.6	6.5	6.2	6.1
Nitrogen [4, 8]	2.31	0.82	0.65	0.09
Sulphur [4, 9]	0.62	0.02	0.02	0.02
Chlorine [4, 9]	0	0.04	0.11	0.02

[1] ISO 5068-2:2007 [2] ISO 562:2010 [3] ISO 1171:2010 [4] ISO 17247:2020 [5] ISO 18134:2016 [6] ISO 18123:2016 [7] ISO 18122:2016 [8] ISO 16948:2015 [9] ISO 16994:2016 [10] By difference.

degree as discussed later in the section 3.1. Regarding nitrogen content, the agricultural residues have a comparable value, but about 7 to 8 times higher than the pine wood one (on a dry basis).

A medium-volatile bituminous coal imported from South Africa was selected to conduct the co-firing tests. The analysis of the coal is also displayed in Table 1. The coal volatiles-to-char ratio is much lower than the biomass ones, while the nitrogen content is significantly higher. The ash content of the coal is in between the values of the two agro-biomasses. All the results shown in Table 1 were provided by an external laboratory of the Spanish National Research Council, whose certified procedures accomplish the respective ISO standards (also included in Table 1). Fuel samples were supplied to that laboratory, where they were independently processed −grounded and sieved− to meet the size specification required by every standard.

The coal and the biomass samples for the oxy-combustion tests were milled, sieved and blended in-house before the experiments were conducted. The mill used was a Retsch ZM200 unit, reducing the fuel size below 250 μm. The milled samples were then processed in a Filtra FTL-200 vibrating sieve sifter; the selected range for coal size was 75–150 μm, while the range chosen for biomasses size was 100–200 μm. These values were prescribed to get a mean residence time of 3 s in the reactor, as explained hereinafter in section 2.3. After the sieving, the different coal + biomass blends were produced in a V-shape rotary mixer. Despite fouling/slagging issues have not been addressed in this investigation, the ash in agro-biomasses could result in a limitation for their potential use in an actual application. For this reason, the biomass shares were limited to 20 % and 50 % to produce the blends.

2.2. Experimental facility

The oxy-combustion tests were carried out in a lab-scale, entrained flow vertical reactor. Drop tube/entrained flow reactors offer the advantages of uniform mixing of the solid- and gas-phase, accurate control of the operating conditions and large versatility for fuel ranks and firing atmospheres. Even though they cannot resemble the complexity of turbulent, swirling flows existing in some large-scale facilities, their use is widely extended to characterize and understand the phenomena occurring during the conversion of pulverized fuels.

Fig. 1 shows the main components of the experimental facility. The reactor is a 2 m long vertical tube with an internal diameter of 0.038 m. The tube is surrounded by four electrical furnaces that can be independently controlled to get a maximum temperature of 1150 °C. The fuel is stored in a hopper and fed to the injector using a screw feeder. The velocity of the screw determines the fuel flow rate supplied and can be controlled by a variable-frequency motor. The injector is water-cooled to avoid fuel conversion before entering the reactor. Mass flow controllers provide O_2 and CO_2 from bottles, while a Coriolis flowmeter provides the water flow rate. A primary stream is used to convey the fuel particles. In contrast, the secondary stream is preheated in four risers inside the electrical furnaces and introduced downwards in the reactor by a straightener.

At the bottom section of the reactor, a sampling probe can be moved up and down to modify the height of the reaction section. N_2 is supplied through this bottom probe, quenching the combustion reactions. After that, a cyclone is used to retain most of the flying solid residues and an ice-cooled condenser is used to remove the moisture in flue gases. Finally, the stream is directed to a gas analyzer, which monitors CO_2, O_2, CO, and NO concentrations. Table 2 summarizes the accuracy of the instruments used for the operation and control of the experimental facility.

Table 2
Accuracy of the instruments in the facility.

Measurement	Accuracy
Feeding gases flow rate (O_2, CO_2, N_2)	± 0.5 %
Feeding water flow rate	± 0.2 %
Temperature	± 2 °C
Pressure	± 3 mbar
Flue gases composition (CO_2, CO, NO)	± 1 %
Flue gases composition (O_2)	± 1.5 %

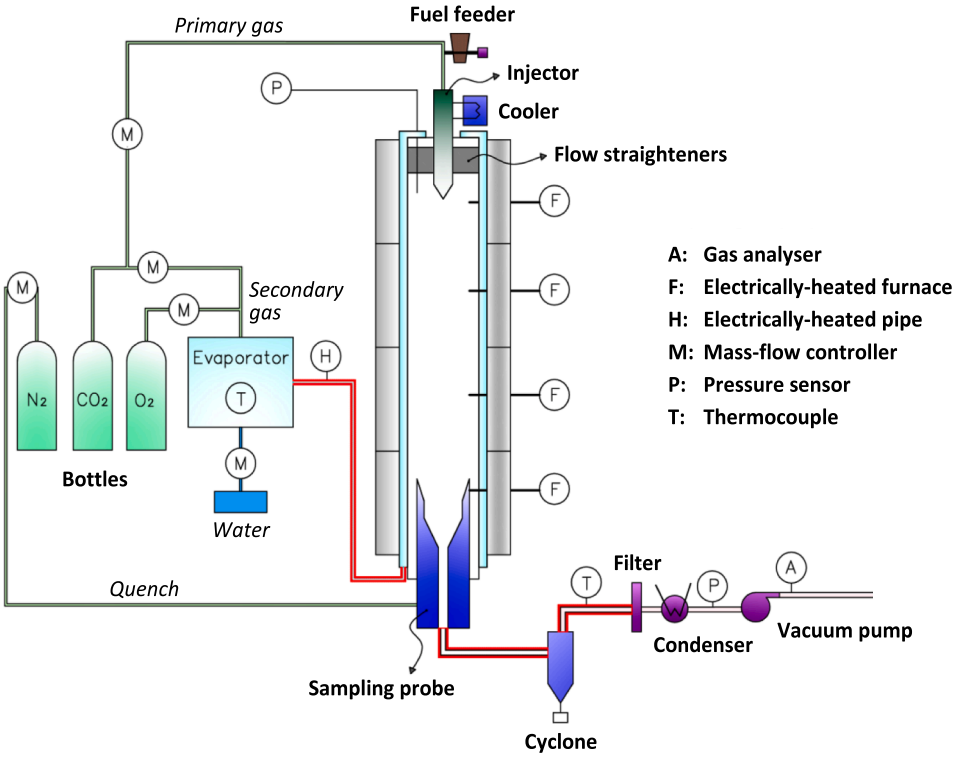

Fig. 1. Diagram of the lab-scale entrained flow reactor.

2.3. Tests campaign

Dry oxy-combustion tests were conducted for two O_2/CO_2 concentrations: 21/79 % and 35/65 %. Furthermore, three H_2O concentrations were used during the wet oxy-combustion tests: 10 %, 25 % and 40 % replacing CO_2 in relation to the dry atmospheres. Thus, a total of 48 tests were carried out during the experimental campaign, i.e. 8 tests for each of the 6 coal + biomass blends. The oxygen excess was kept the same for all the tests, with an oxygen ratio $\lambda = 1.25$ (available O_2/stoichiometric O_2). The initial reactor temperature was kept the same for all the oxy-combustion tests, set at 1000 °C. This value is well above the ignition temperature of the fired blends, enabling the fuels to be converted as soon as they enter the reaction section. Once the temperature reaches the set-point, fuel-feeding stars and stable operation is rapidly achieved after a short transient period. The steadiness is assessed through several online available measurements: power consumption of the electrical furnaces and flue gas composition at the reactor exit. All the results presented and discussed later in sections 3.2 and 3.3 have been obtained from at least 240 operating data sets per blend and firing atmosphere. The criterion adopted to evaluate the operation stability was a maximum relative standard deviation of 3 % of the mean value for the power consumptions of the four electrical furnaces and the O_2 and CO_2 contents in flue gases at the reactor outlet for all operating data sets.

Tables 3 and 4 show the fuel mass flow rates and the O_2, CO_2, and H_2O mass flow rates used during the tests. These flow rates were computed to get a mean residence time of 3 s for all the tests, setting the height of the reaction section at 1.5 m. The mean residence time is estimated by dividing the reactor height by the velocity of a mean-size particle. The maximum velocity has two contributions: on the one hand, the terminal velocity of a falling solid in a fluid and, on the other hand, the drag velocity caused by the entraining gases. Since the coal-to-biomass density ratio ρ_C/ρ_B is around 1.95, the coal-to-biomass size ratio d_C/d_B should be $(1 / 1.95)^{0.5} \approx 0.72$ to get the same terminal velocity, according to Stokes' law for low Reynolds numbers. This is the rationale behind the different size ranges selected for the coal and the biomasses, previously presented in section 2.1. As concerns the drag velocity, complete releases of mass and heat from the fuel are assumed to estimate the flue gas volumetric flow rates, since they are unknown *ab initio* when defining the test conditions. As discussed in detail by An et al. [46], CFD-based tools provide more realistic estimates of residence times for entrained flow reactors than idealized plug flow models, with differences up to 30 % in particle velocities. At least, adopting the same calculation hypotheses for the flow rates shown in Tables 3 and 4 can be deemed a reasonable approach, enabling a reliable comparison of the experimental results.

The O_2, CO_2, and H_2O flow rates during the tests were measured and recorded online during every test execution in order to check that the prescribed values were supplied to the reactor. The accuracy of the flow meters has already been presented in Table 2. The measurement of the fuel flow rate was not available online during the tests, but the frequency of the motor driving the screw feeder was (calibrated before every test running to relate the fuel flow rate with the frequency). An averaged value for the actual fuel flow rate can be obtained from the weight difference of the solids in the hopper before and after every test, and then a percentage deviation can be computed by means of Eq. (1):

$$\varepsilon(\%) = 100\frac{\dot{m}_{fuel,actual} - \dot{m}_{fuel,expected}}{\dot{m}_{fuel,expected}} \quad (1)$$

Table 5 summarizes the percentage deviations ε between the averaged, actual fuel flow rates and the expected fuel flow rates (those shown in Tables 3 and 4) for all the tests included in the experimental campaign. All the deviations are small, in the range (−2.2 %, 3.1 %), and do not show any systematic trend. According to this information, the accuracy of the fuel flow rates can be deemed reliable enough to proceed with the discussion of the results.

Finally, solid samples collected in the cyclone at the reactor cold end section were processed to obtain the fuel burnout for each experimental condition, that is, the solid-to-gas conversion ratio. The unburned fuel and ashes contents in those collected solids were determined in a Hobersal HD230 muffle oven, as the weights of the raw, dry and burned samples were obtained in Ohaus Pioneer precision balance with an accuracy of ± 0.0001 g. The burnout β can be calculated according to the ash-tracer method, Eq. (2), where α stands for the ash content on a dry basis:

$$\beta = \frac{\alpha_{cyclone} - \alpha_{fuel}}{\alpha_{cyclone}\left(1 - \alpha_{fuel}\right)} \quad (2)$$

3. Results and discussion

3.1. Burnout

The values of the burnout degrees obtained during the dry oxy-combustion tests are presented in Table 6 for all the blends fired and the two O_2 concentrations (21 % and 35 %). Enriching the O_2 content in the firing atmosphere means a higher partial pressure of the oxidant, which enhances the O_2 diffusion in the gas-phase, increasing the volatile oxidation rates and raising the temperature levels. Char conversion is also influenced by the increments of both the particle temperature and the O_2 diffusivity. According to the values shown in Table 6, the use of 20 % agro-biomasses reduces the burnout in comparison to the co-firing of 20 % pine wood, consistently with their lower volatiles-to-char ratios (since all the tests were carried out keeping the same mean residence time, as explained before in section 2.3). For the 20 % biomass share, the burnout differences between the three types of biomass are diminished when the atmosphere is enriched in O_2: from 0.97 and 2.36 percentage points to 0.73 and 1.13 percentage points, respectively. This behavior is explained by a slightly higher increment of the char conversion of the agro-biomasses, provided that their char contents are higher and all the volatiles are released given the experimental conditions during the tests.

When the biomass share in the blend is raised from 20 % to 50 %, burnout degrees are increased by around 10 percentage points for the 21 % O_2 cases and around 3.7 percentage points for the 35 % O_2 cases. This is mainly related to the larger volatiles-to-char ratios of the resulting blends and the higher char porosity of the biomasses in relation to coal [24]. The values obtained when co-firing 50 % coal + 50 %

Table 3
Mass flow rates during the combustion tests of the 80 % coal + 20 % biomass blends.

Atmosphere (% vol.)	**Fuel flow rate** (g/min)			**O_2 flow rate** (g/min)			**CO_2 flow rate** (g/min)			**H_2O flow rate** (g/min)		
	C + P	C + A	C + V	C + P	C + A	C + V	C + P	C + A	C + V	C + P	C + A	C + V
21/79 O_2/CO_2	0.59	0.59	0.59	1.38	1.38	1.38	7.13	7.13	7.15	0	0	0
21/69/10 O_2/CO_2H_2O	0.59	0.59	0.59	1.38	1.38	1.38	6.23	6.23	6.25	0.37	0.37	0.37
21/54/25 O_2/CO_2H_2O	0.59	0.59	0.59	1.38	1.38	1.38	4.87	4.87	4.89	0.92	0.92	0.93
21/39/40 $O_2/CO_2/H_2O$	0.59	0.59	0.59	1.38	1.38	1.38	3.52	3.52	3.53	1.48	1.48	1.49
35/65 O_2/CO_2	0.95	0.95	0.95	2.23	2.23	2.24	5.69	5.69	5.71	0	0	0
35/55/10 $O_2/CO_2/H_2O$	0.95	0.95	0.95	2.23	2.23	2.24	4.81	4.81	4.83	0.36	0.36	0.36
35/40/25 $O_2/CO_2/H_2O$	0.95	0.95	0.95	2.23	2.23	2.24	3.50	3.50	3.52	0.89	0.89	0.90
35/25/40 $O_2/CO_2/H_2O$	0.95	0.95	0.95	2.23	2.23	2.24	2.19	2.19	2.20	1.43	1.43	1.44

Table 4
Mass flow rates during the combustion tests of the 50 % coal + 50 % biomass blends.

Atmosphere (% vol.)	**Fuel flow rate** (g/min)			**O_2 flow rate** (g/min)			**CO_2 flow rate** (g/min)			**H_2O flow rate** (g/min)		
	C + P	C + A	C + V	C + P	C + A	C + V	C + P	C + A	C + V	C + P	C + A	C + V
21/79 O_2/CO_2	0.65	0.66	0.66	1.35	1.35	1.36	6.98	6.98	7.04	0	0	0
21/69/10 O_2/CO_2H_2O	0.65	0.66	0.66	1.35	1.35	1.36	6.10	6.10	6.15	0.36	0.36	0.36
21/54/25 O_2/CO_2H_2O	0.65	0.66	0.66	1.35	1.35	1.36	4.77	4.77	4.81	0.90	0.90	0.91
21/39/40 $O_2/CO_2/H_2O$	0.65	0.66	0.66	1.35	1.35	1.36	3.45	3.45	3.48	1.45	1.45	1.46
35/65 O_2/CO_2	1.04	1.06	1.06	2.15	2.15	2.18	5.50	5.50	5.57	0	0	0
35/55/10 $O_2/CO_2/H_2O$	1.04	1.06	1.06	2.15	2.15	2.18	4.66	4.66	4.71	0.35	0.35	0.35
35/40/25 $O_2/CO_2/H_2O$	1.04	1.06	1.06	2.15	2.15	2.18	3.39	3.39	3.43	0.87	0.87	0.88
35/25/40 $O_2/CO_2/H_2O$	1.04	1.06	1.06	2.15	2.15	2.18	2.12	2.12	2.14	1.39	1.39	1.40

Table 5
Percentage deviations (%) between the averaged, actual fuel flow rates and the expected fuel flow rates.

Atmosphere (% vol.)	80C + 20P	80C + 20A	80C + 20V	50C + 50P	50C + 50A	50C + 50V
21/79 O_2/CO_2	−1.4	2.5	−1.7	1.9	3.1	−1.4
21/69/10 O_2/CO_2H_2O	1.9	−1.9	−1.8	1.8	−1.9	1.1
21/54/25 O_2/CO_2H_2O	2.3	2.0	1.2	−0.9	1.5	−2.2
21/39/40 $O_2/CO_2/H_2O$	−1.8	1.8	−1.8	1.1	−1.1	−2.0
35/65 O_2/CO_2	1.5	−1.9	−1.8	−1.8	2.0	−1.2
35/55/10 $O_2/CO_2/H_2O$	−1.2	1.3	2.4	1.5	−1.3	2.5
35/40/25 $O_2/CO_2/H_2O$	−0.9	−2.1	2.2	2.3	1.7	1.2
35/25/40 $O_2/CO_2/H_2O$	−1.9	1.1	1.2	−1.7	−2.2	2.7

Table 6
Burnout degrees (%) under O_2/CO_2 atmospheres: effect of the biomass type and share in the blend.

Atmosphere (% vol.)	80C + 20P	80C + 20A	80C + 20V	50C + 50P	50C + 50A	50C + 50V
21/79 O_2/CO_2	83.67	82.70	81.31	93.55	92.64	91.63
35/65 O_2/CO_2	93.34	92.61	92.21	97.01	96.33	95.97

biomass under the 35 % O_2 atmosphere point to a good performance of the agro-biomasses in relation to the pine wood: 97.01 % vs 96.33 % when pine wood is replaced with the blend of vineyard + corn, and 97.01 % vs 95.97 % when pine wood is replaced with the raw vineyard pruning. These burnout levels do not represent a final conversion limit for the fuels and blends fired, rather being the achieved burnout degrees for every specific experimental condition during the tests in the reactor.

Fig. 2 shows the effect of replacing CO_2 with H_2O (10–40 %) on the burnout degree of the six coal and biomass blends for the 21 % O_2 tests. For clarity, the scale of the ordinate axis in the left and right plots of Fig. 2 is not the same. Notwithstanding the different extent of the burnout variation caused by the steam addition, the observed trends are very similar regardless of the type of biomass and its share in the blend. When CO_2 is replaced with H_2O, solid-to-gas conversion rises due to increased flame temperature and oxygen availability [47]. The former is because of the lower heat capacity of steam, and the latter is because the oxidant diffusivity in steam is higher (both in comparison to CO_2).

Nevertheless, the burnout increments caused by the steam are not proportional to its concentration, and an evident attenuation is observed when shifting from 25 % H_2O to 40 % H_2O. A similar behavior can be

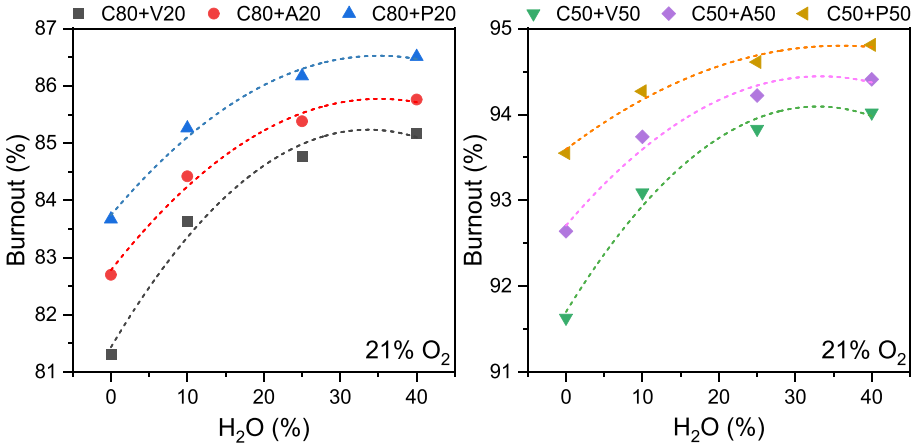

Fig. 2. Burnout degrees for the 21 % O_2 tests: effects of the biomass type and the CO_2 replacement by H_2O. Left plot: 80 % coal + 20 % biomass; right plot: 50 % coal + 50 % biomass.

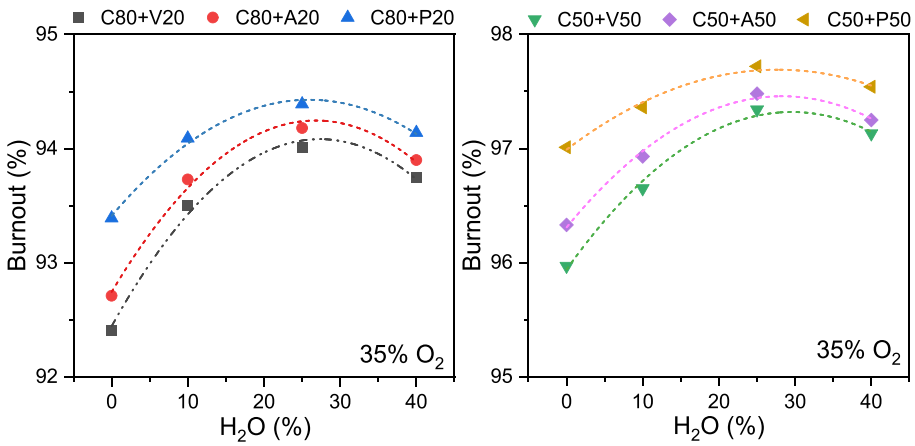

Fig. 3. Burnout degrees for the 35 % O_2 tests: effects of the biomass type and the CO_2 replacement by H_2O. Left plot: 80 % coal + 20 % biomass; right plot: 50 % coal + 50 % biomass.

Table 7
BET specific surface areas (m^2/g): effect of CO_2 replacement by H_2O.

Atmosphere (% vol.)	50C + 50P	50C + 50A	50C + 50V
21/79 O_2/CO_2	234.9	216.7	227.9
21/39/40 $O_2/CO_2/H_2O$	202.6	182.9	191.1
35/65 O_2/CO_2	221.2	204.8	217.9
35/25/40 $O_2/CO_2/H_2O$	170.0	155.6	160.3

observed in Fig. 3, where the effect of replacing CO_2 with H_2O (10–40 %) on the burnout degree is represented for the 35 % O_2 cases. Indeed, a decrease in burnout is detected in Fig. 3 for the 40 % H_2O cases compared to the 25 % H_2O ones, regardless of the type and share of biomass in the blend. The 35/25 % O_2/H_2O atmosphere leads to the maximum burnout values along with the minimum differences whether agro-biomass is used instead of pine wood: 97.72 % vs 97.48 % when replacing 50 % of pine wood by the blend of vineyard + corn, 97.72 % vs 97.34 % when replacing 50 % of pine wood by the raw vineyard pruning.

Some published experiences [38,48] have reported a similar behavior to that shown in Fig. 3, finding a particular steam concentration maximizing fuel conversion and minimizing emissions during the wet oxy-combustion of coal. In particular, char-specific surface areas can be affected when large steam concentrations are used in the atmosphere [49,50]. To confirm this influence, a collection of solid samples taken from the cyclone was selected to determine the BET-specific surface areas of the chars. The results obtained are shown in Table 7. The determination was done by means of N_2 isothermal adsorption at 77 K, with previous degassing of the samples at 250 °C during 5 h. The specific surface areas were estimated, assuming that the fraction of ashes in the samples had negligible porosity. According to the values presented in Table 7, a significant decrease in the BET-specific surface areas is detected when replacing 40 % CO_2 with H_2O compared to the dry tests. The extent of the reduction is larger for the 35 % O_2 cases since the CO_2 replacement ratio is higher than in the 21 % O_2 tests (40 % out of 65 % vs 40 % out of 79 %). This diminution of the reactive surface areas of the chars could affect the solid-to-gas conversion rates, explaining the trends observed in Figs. 2 and 3. Nevertheless, considering the dry atmospheres as the reference cases, adding 10–40 % H_2O as CO_2 replacement always increases the burnout degrees for the two O_2 concentrations and the six coal + biomass blends.

3.2. C-fuel conversion to CO

It is worth also seeking the fraction of C-fuel that has been released to the gas phase but partially oxidized to CO and not completely to CO_2. For this purpose, the mean values and standard deviations of the C-fuel to CO conversion degrees are represented in Figs. 4 and 5 for all the experimental conditions. Fig. 4 shows the results obtained for the three 80 % coal + 20 % biomass blends, whereas Fig. 5 shows the results for the three 50 % coal + 50 % biomass blends. The conversion degrees can be calculated from the closure of the carbon mass balance, provided that inlet mass flow rates of fuel and gases are known, as well as the fuel ultimate analysis and the CO and CO_2 concentrations in flue gases

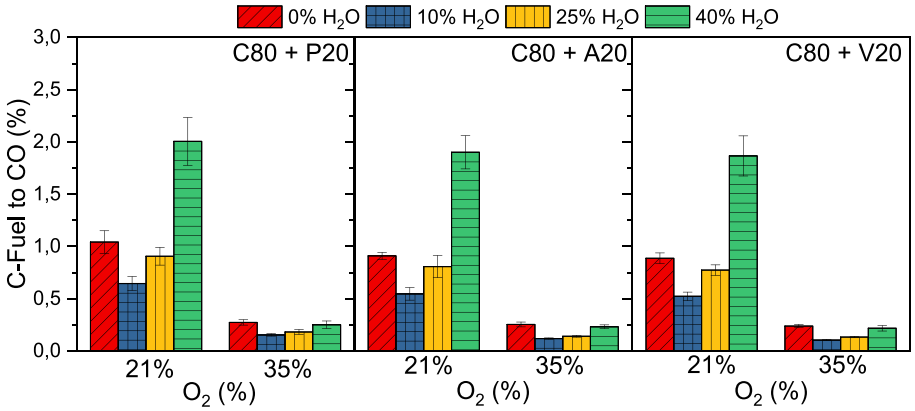

Fig. 4. C-fuel to CO conversions for the 80 % coal + 20 % biomass blends: effects of the biomass type and the CO_2 replacement by H_2O.

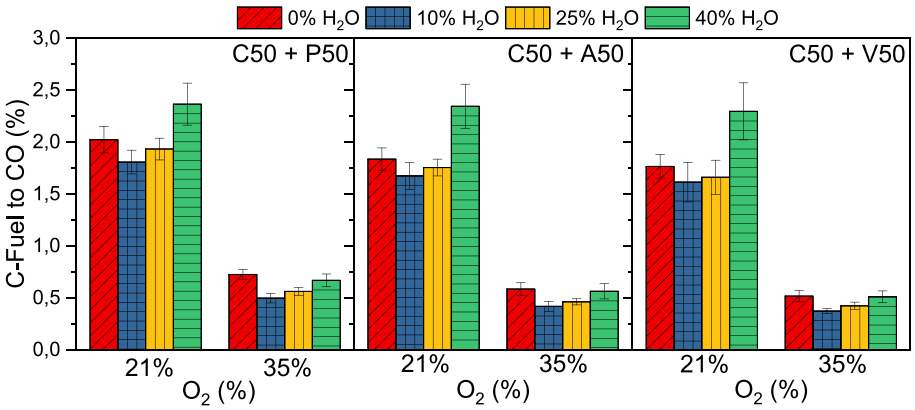

Fig. 5. C-fuel to CO conversions for the 50 % coal + 50 % biomass blends: effects of the biomass type and the CO_2 replacement by H_2O.

Table 8
N-fuel to NO conversion (%) under O_2/CO_2 atmospheres: effects of the biomass type and share in the blend.

	80C + 20P	80C + 20A	80C + 20V	50C + 50P	50C + 50A	50C + 50V
Atmosphere (% vol.)						
21/79 O_2/CO_2	11.94 ± 0.24	14.07 ± 0.17	16.40 ± 0.19	10.19 ± 0.11	12.51 ± 0.10	14.62 ± 0.12
35/65 O_2/CO_2	14.19 ± 0.19	16.11 ± 0.16	18.05 ± 0.21	12.37 ± 0.14	14.66 ± 0.11	16.50 ± 0.14
Nitrogen content in the blend (% wt., dry basis)	1.87	1.98	2.01	1.20	1.48	1.57
Volatiles-to-char ratio in the blend (% wt.)	1.27	0.91	0.76	2.62	1.73	1.36

leaving the reactor.

According to the results shown in Figs. 4 and 5, the less influential factor in the C-fuel to CO conversion degrees is the type of biomass used in the blend. For every specific O_2/H_2O atmosphere and biomass share ratio, the differences between the three types of biomass are very narrow. The maximum CO levels are linked to the use of pine wood, which was also the biomass showing the largest burnout rates in the previous section. However, the agro-biomasses offer very similar C-fuel to CO values. When the biomass share in the blend is raised from 20 % to 50 %, the CO levels are always higher: increments in the range 0.26–1.09 percentage points in the case of the pine wood, 0.29–1.13 percentage points in the case of the vineyard + corn blend, and 0.30–1.15 percentage points in the case of the raw vineyard pruning. These numbers have to be again related to the burnout ratios presented in section 3.1: the larger the coal share replaced with biomass, the higher the solid-to-gas conversions obtained. This eventually means a higher CO release from the heterogeneous C-char oxidation, which is not totally oxidized to CO_2 along the reactor height.

The effect of O_2 enrichment in the atmospheres from 21 % to 35 % can be clearly seen in Figs. 4 and 5, with a significant reduction of the CO levels for all the blends. For the 35 % O_2 atmospheres, C-fuel to CO conversions are always below 0.27 % when co-firing 20 % biomass and below 0.73 % when co-firing 50 % biomass. The larger O_2 availability promotes CO oxidation to CO_2, thus reducing the CO detected in the flue gases at the reactor exit in comparison to the 21 % O_2 atmospheres. Burnout and C-fuel to CO conversion degrees are not only influenced by the O_2 concentration, but also by the oxygen excess and the oxygen staging, as shown by Riaza et al. [47] and Escudero et al. [51] for pulverized fuel conditions, and by Lupiáñez et al. [52] and Sher at al. [53] for fluidized bed conditions.

The effect of CO_2 replacement by H_2O on the C-fuel to CO conversion degree can also be seen in Figs. 4 and 5. For the 21 % O_2 cases, the addition of 10 % H_2O diminishes the CO levels to a larger extent for the blends with 20 % biomass. This CO reduction is related to the higher O_2 diffusivity in H_2O. Nevertheless, the trend is reversed when adding larger amounts of steam, resulting in a significant CO increase for the 40 % H_2O tests compared to the dry ones: around 2 times for the 20 % biomass blends and 1.25 times for the 50 % biomass blends. The steam induces more intense char gasification, and larger CO rates are released in the particle proximity; for the largest H_2O concentrations, some of that additional formed CO cannot be oxidized before the quenching at the reactor outlet. The same effect caused by the steam is observed for the 35 % O_2 cases in Figs. 4 and 5. However, the extent of the C-fuel to CO variations is much more limited since gasification is attenuated for high O_2 concentrations [49]. In these cases, the CO levels for the 0 % and 40 % H_2O contents are of comparable value.

3.3. N-fuel conversion to NO

NO_x formation from solid fuel oxy-combustion is primarily due to the oxidation of the nitrogen bound in the fuel, either homogeneously in the gas-phase (N-volatiles released) or heterogeneously in the solid N-char. This is the so-called NO_x-fuel mechanism, mainly controlled by the O_2 concentration in the oxidizing atmosphere, with NO being the majority compound formed [54]. According to the fuel analysis shown in Table 1, an increase in NO_x formation should be expected when the agro-biomasses are fired instead of the wood pine, whose nitrogen content is significantly lower. Table 8 shows the mean values and standard deviations of the N-fuel conversion to NO for the six blends of coal + biomass and the two dry atmospheres. These conversion degrees can be calculated from the available NO concentration in the flue gases at the reactor exit. For the sake of clarity, the information about the nitrogen content and the volatiles-to-char ratios for the six blends are also included in Table 8 (that can be calculated from the information previously shown in Table 1).

The effect of enriching the O_2 concentration from 21 % to 35 % can be well seen in the results of Table 8: for every specific biomass type and share in the blend, there is an increase of the NO formed. The N-fuel to NO conversion values for the 35 % O_2 cases range 1.1–1.2 times the values obtained for the 21 % O_2 tests. This influence can be different under fluidized bed oxy-combustion, since the temperature levels are significantly lower than the existing under pulverized fuel combustion. Sher et al. [55] tested two non-woody fuels (miscanthus and straw pellets) and one woody fuel (domestic wood pellet) in a 20 kW_{th}

bubbling fluidized bed combustor, under air and oxy-fuel combustion conditions. NO_x emissions were found to decrease when switching from 25 % to 30 % O_2, mainly due to the rise of the bed temperature and the consequent enhancement of the N-volatiles release in the dense zone; the formed NO was partially depleted later in the freeboard. The temperatures in the freeboard depended on the biomass type, being a dominant variable affecting both the CO and the NO emissions. The results can be however different in circulating fluidized beds. Kosowska et al. [56] tested three kinds of biomass (agro, woody and energy crop) in a lab-scale oxy-fired CFB reactor. Maximum NO formation was detected for 40 % O_2 atmospheres, explained by the intensified oxidation of both the N-volatiles and the N-char along the riser.

The effect of the nitrogen content in the blends is also perceptible in the results shown in Table 8: the replacement of the same fraction (20 % or 50 %) of pine wood by the agro-biomasses increases the N-fuel to NO conversion degrees, for every specific O_2 concentration. Nevertheless, the increments observed when co-firing the raw vineyard pruning (ranging from 3.86 to 4.46 percentage points) are significantly higher than the obtained when co-firing the vineyard + corn blend (1.92–2.32 percentage points) even though its nitrogen content is not proportionally so high. This behavior can be related to the different volatiles-to-char ratios of the selected agro-biomasses. The NO formed by the fast oxidation of the N-volatiles (HCN, NH_3) can be partially depleted by interactions with other volatile species, mainly light hydrocarbons [44]. This reduction mechanism barely involves the NO formed from the direct oxidation of the N-char since this heterogeneous reaction is slower. Then, the release is more evenly distributed along the reactor height. Finally, as for the effect of increasing the biomass share in the blend, not-so-meaningful insights can be obtained from Table 8. A decrease in N-fuel to NO conversion is detected. However, the comparison is not straightforward since the burnout degrees are appreciably different when using 20 % or 50 % of the biomass in the blend.

The replacement of CO_2 by H_2O in the atmosphere also affects the N-fuel to NO conversion degrees due to their different thermo-physical properties and the steam's active role in some NO depletion mechanisms. On the one hand, the flame temperature and O_2 diffusivity are higher when H_2O replaces CO_2, which would enhance the NO formation. On the other hand, H_2O is known to promote or participate in several reactions competing with HCN and NH_3 oxidation to form NO. The main set of reactions is presented in Table 9, summarized as follows: 1) HCN depletion in the gas phase, competing with HCN oxidation and reducing NO with NH_3, (R.1), (R.2) and (R.3); 2) HCN depletion in the gas-phase by [OH] and [H] radicals from the steam, competing with HCN oxidation, (R.4) and (R.5); 3) NO depletion in the gas-phase by CO, due to the more intense char gasification caused by the steam, (R.6); 4) NO heterogeneous depletion with carbon-free sites in the solid surface, also promoted by the enhanced char gasification, (R.7).

The mean values of the N-fuel to NO conversions are depicted in Fig. 6 for the six blends and the two O_2 concentrations when replacing CO_2 with H_2O in the range 10–40 %. For the three 80 % coal + 20 % biomass blends, the addition of 10 % H_2O diminishes the NO formation to a similar extent for the two O_2 concentrations and slightly higher for the two agro-biomasses: relative reductions of 8.5–9.4 % when using pine wood, 9.6–10.7 % for the corn + vineyard blend, 11–12.2 % for the raw vineyard pruning. A larger addition of steam, from 10 % to 25 %, further reduces the N-fuel conversion to NO, but to a more limited extent and not proportional to the steam concentration. Finally, when using 40 % H_2O as CO_2 replacement, the trend is reversed, pointing to the occurrence of a steam concentration minimizing the N-fuel to NO conversion degree. This is consistent with previous experiences [17,38] claiming a fuel-NO_x intensification for large steam concentrations with some dependence on the fuel rank. Indeed, the reducing effect of the H_2O in Fig. 6 is more limited when co-firing 50 % coal + 50 % biomass, resulting in smoother variations as the volatile-to-char ratio in the blend is increased.

Table 9
Chemical reactions contributing to NO depletion for wet oxy-combustion of solid fuels.

Reaction	Reference
(R.1) $HCN + H_2O \rightarrow NH_3 + CO$	[57]
(R.2) $NH_3 + NO + \frac{1}{4}O_2 \rightarrow N_2 + \frac{3}{2}H_2O$	[58,59]
(R.3) $NH_3 + \frac{3}{2}NO \rightarrow \frac{5}{4}N_2 + \frac{3}{2}H_2O$	[58,59]
(R.4) $HCN + H \leftrightarrow H_2 + CN$	[44]
(R.5) $HCN + OH \leftrightarrow H_2O + CN$	[44]
(R.6) $CO + NO \rightarrow \frac{1}{2}N_2 + CO_2$	[60]
(R.7) $C_{char} + NO \rightarrow \frac{1}{2}N_2 + CO$	[61]

To clearly see the comparison between the dry and wet atmospheres, Fig. 7 represents the accumulative percentage reduction of N-fuel conversion to NO caused by steam, using the dry atmosphere as the reference value. Several outcomes can be obtained from the results in Fig. 7: 1) the addition of 10–40 % H_2O as CO_2 replacement always reduces NO formation in comparison to the dry atmospheres for the cases tested; 2) the larger the volatiles-to-char ratio in the blend, the lower the NO reducing effect caused by the steam in comparison to the dry atmospheres; 3) minimum NO formation is always detected for the 25 % H_2O concentration, but seeming that this value would tend to be lowered as the volatiles-to-char ratio would increase (for the 50 % coal + 50 % pine wood blend, the differences between the 10 % and 25 % H_2O cases are the lowest ones). These results confirm that, beyond a particular H_2O concentration, the effects of the NO-reducing mechanisms in which steam is involved are partially compensated by the enhancement of N-fuel oxidation.

4. Conclusions

The oxy-combustion of blends of coal and two types of agro-waste biomass has been experimentally characterized and compared to typical pine wood under a combination of dry and wet conditions. The experiments were conducted in an entrained flow reactor, keeping the same initial temperature, oxygen excess, and mean residence time for all the tests. Both the fuel sizes and the operating conditions suitably resemble the actual performance that would be occurring in a larger-scale facility. Two biomass shares, 20 % and 50 % on a mass basis, have been selected. The six coal + biomass blends have been fired for a combination of atmospheres, encompassing two O_2 concentrations (21 %, 35 %) and four H_2O concentrations (0 %, 10 %, 25 %, 40 %), aiming at providing novel results towards the concept of oxy-steam combustion.

The focus has been put on the combustion characteristics that would be more challenging concerning the use of agro-waste biomasses, i.e., fuel conversion efficiency and NO formation. As for the burnout degree, outstanding performance of the two agro-waste biomasses has been obtained for the 35 % O_2 cases: up to 97.48 % for 50 % coal + 50 % vineyard and corn, and 97.34 % for 50 % coal + 50 % raw vineyard pruning, with minimum differences of 0.24 and 0.38 percentage points below the obtained with 50 % coal + 50 % pine wood. Another of the new findings of the work is the steam concentration that maximizes the burnout degree. In most of the cases, 25 % H_2O atmospheres have resulted in higher solid-to-gas conversions than the observed for 40 % H_2O. This result is related to the reduction of the char-specific surface areas, which partially offsets the effect caused by H_2O as for the rise of the flame temperature and the O_2 diffusivity.

No significant influences of the type of biomass have been detected on the incomplete C-char combustion, i.e. the fraction of CO produced instead of CO_2. For the 21 % O_2 cases, the rise of the biomass shares from 20 % to 50 % in the blend increases C-fuel to CO conversion in the range of around 0.3–1.2 percentage points, while the addition of 40 % H_2O largely intensifies char gasification, doubling the CO levels in comparison to the dry cases. This effect is very much attenuated for the 35 % O_2

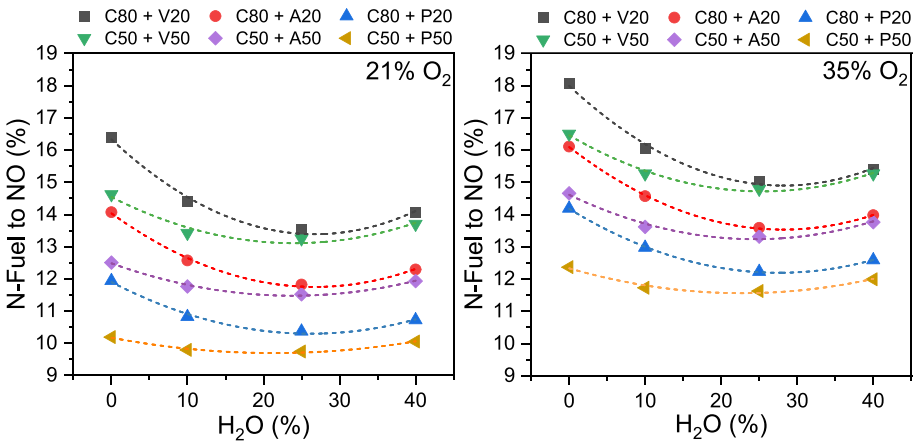

Fig. 6. N-fuel to NO conversions under O_2/CO_2 and $O_2/CO_2/H_2O$ atmospheres: effects of the biomass type and the CO_2 replacement by H_2O. Left plot: 21 % O_2; right plot: 35 % O_2.

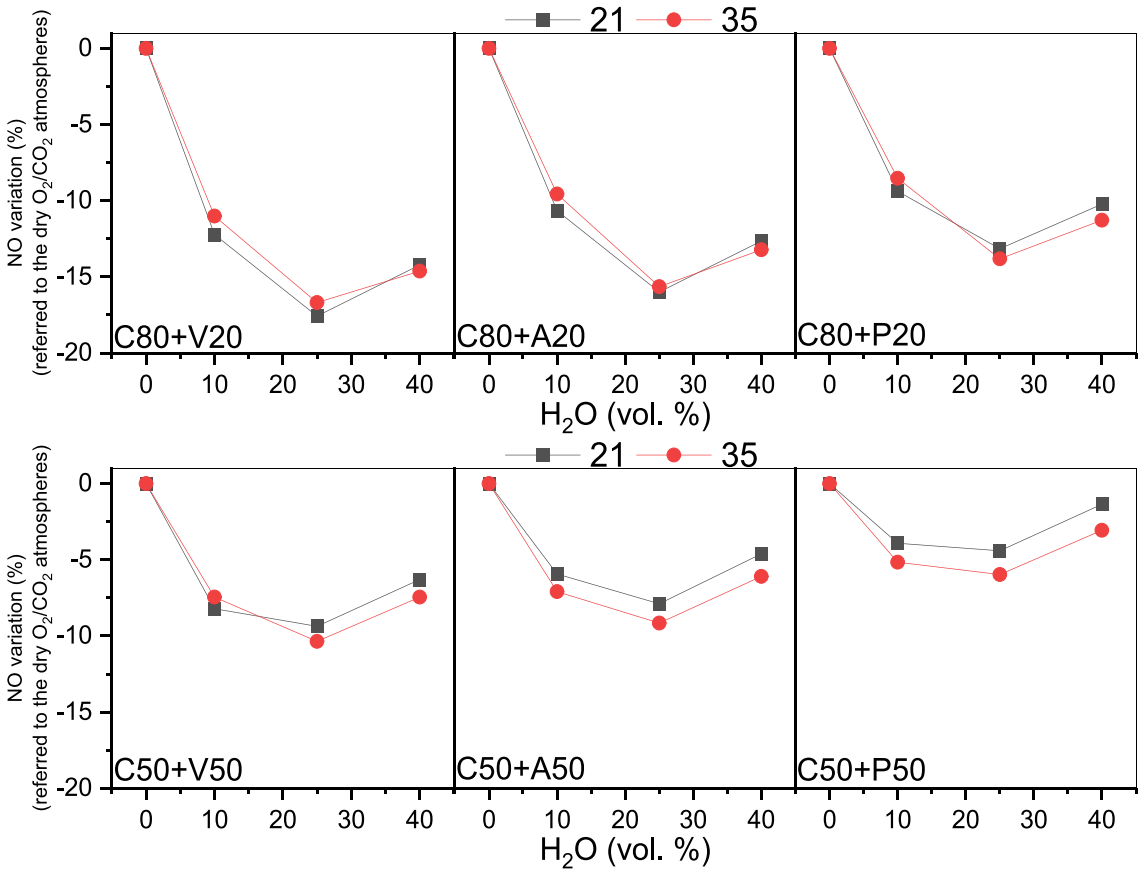

Fig. 7. Accumulative variations (%) in fuel-N to NO conversion rates for different H_2O concentrations. Top plot: blends of 80 % coal + 20 % biomass; bottom plot: blends of 50 % coal + 50 % biomass.

cases when the C-fuel to CO conversions are always below 0.27 % and 0.73 % for the 20 % and 50 % biomass shares, respectively.

Concerning the NO formation, it is concluded that the larger the agro-waste biomass in the share, the higher the N-fuel to NO conversion. This is consistent with the fuel-NO_x mechanism, depending on the nitrogen content in the solid fuel. Compared to the use of pine wood, N-fuel to NO conversion degree significantly increases, up to 22.7 % when using corn + vineyard and up to 43.4 % when using the raw vineyard pruning for the dry atmospheres. CO_2 replacement by H_2O is detected to reduce the N-fuel to NO conversion, with the most significant decrements for the 25 % H_2O cases: −17.6 % for the blends with pine wood, −16 % for the blends with corn + vineyard, and −13.8 % for the blends with raw vineyard pruning. The extent of these reductions is lower for the blends with higher volatile contents, which is also a remarkable insight. The N-volatile oxidation is enhanced for the largest steam concentrations, counterbalancing the steam-induced NO depletion.

Concluding, the experimental research has led to a new, comprehensive characterization of the dry and wet oxy-combustion performance of blends with non-conventional biomasses. The effects of the

biomass types and shares have been assessed, as well as the atmospheres maximizing fuel conversions and minimizing NO formation. In particular, wet oxy-combustion should be preferable due to the increase in combustion efficiency and the reduction of NO compared to dry oxy-combustion. The findings presented in this work highlight the potential applicability of the selected agro-waste biomasses. However, additional research would still be needed to address other issues, mainly related to slagging/fouling phenomena.

CRediT authorship contribution statement

Luis I. Díez: Writing – original draft, Methodology, Investigation, Funding acquisition, Conceptualization. **Alexander García-Mariaca:** Writing – original draft, Validation, Investigation. **Eva Llera-Sastresa:** Writing – original draft, Validation, Methodology, Investigation. **Paula Canalís:** Writing – original draft, Validation, Methodology, Investigation.

Declaration of competing interest

The authors declare that they have no known competing financial interests or personal relationships that could have appeared to influence the work reported in this paper.

Data availability

Data will be made available on request.

Acknowledgements

The work described in this study was co-funded by the National Research Program from the Spanish Ministry of Science and Innovation, under the Project RTI2018-094488, and the European Funds for Regional Development.

References

[1] Na H, Sun J, Qiu Z, Yuan Y, Du T. Optimization of energy efficiency, energy consumption and CO_2 emission in typical iron and steel manufacturing process. Energy 2022;257:124822. https://doi.org/10.1016/j.energy.2022.124822.
[2] Sahoo N, Kumar A, Samsher. Review on energy conservation and emission reduction approaches for cement industry. Environ Dev 2022;44(100767). https://doi.org/10.1016/j.envdev.2022.100767.
[3] Yin C, Qiu S, Zhang S, Sher F, Zhang H, Xu J, et al. Strength degradation mechanism of iron coke prepared by mixed coal and Fe_2O_3. J Anal Appl Pyrol 2020;150:104897. https://doi.org/10.1016/j.jaap.2020.104897.
[4] Loo DL, Teoh YH, How HG, Le TD, Nguyen HT, Rashid T, et al. Effect of nanoparticles additives on tribological behaviour of advanced biofuels. Fuel 2023;334:126798. https://doi.org/10.1016/j.fuel.2022.126798.
[5] Wu H, Li A, Gao S, Xing Z, Zhao P. The performance, mechanism and greenhouse gas emission potential of nitrogen removal technology for low carbon source wastewater. Sci Total Environ 2023;903:166491. https://doi.org/10.1016/j.scitotenv.2023.166491.
[6] Zhang L, Jiang G, Xiao R, Hou K, Liu X, Liu X, et al. An appropriate amount of straw replaced chemical fertilizers returning reduced net greenhouse gas emissions and improved net ecological economic benefits. J Clean Prod 2024;434:140236. https://doi.org/10.1016/j.jclepro.2023.140236.
[7] Rashid T, Sher F, Jusoh M, Joya TA, Zhang S, Rasheed T, et al. Parametric optimization and structural feature analysis of humic acid extraction from lignite. Environ Res 2023;220(115160). https://doi.org/10.1016/j.envres.2022.115160.
[8] Wall T, Liu Y, Spero C, Elliot L, Khare S, Rathman R, et al. An overview on oxyfuel coal combustion - State of the art research and technology development. Chem Eng Res Des 2009;87:1003–16. https://doi.org/10.1016/j.cherd.2009.02.005.
[9] Yin C, Yan J. Oxy-fuel combustion of pulverized fuels: combustion fundamentals and modeling. Appl Energy 2016;162:742–62. https://doi.org/10.1016/j.apenergy.2015.10.149.
[10] Raho B, Colangelo G, Milanese M, de Risi A. A critical analysis of the oxy-combustion process: from mathematical models to combustion product analysis. Energies (Basel) 2022;15:6514. https://doi.org/10.3390/en15186514.
[11] Ling JLJ, Yang W, Park HS, Lee HE, Lee SH. A comparative review on advanced biomass oxygen fuel combustion technologies for carbon capture and storage. Energy 2023;284:128566. https://doi.org/10.1016/j.energy.2023.128566.
[12] Wang R, Liu Z, Song X, Liu S. Co-combustion of pulverized coal and walnut shells in air and oxy-fuel atmospheres: Thermal behavior, synergistic effect and kinetics. J Energy Inst 2023;108:101243. https://doi.org/10.1016/j.joei.2023.101243.
[13] Bai C, Zhang Y, Zhang W, Chen K, Deng L, Zhao Y, et al. Experimental study on the structure and reactivity of char in pressurized O_2/H_2O atmosphere. Fuel Process Technol 2022;237:107469. https://doi.org/10.1016/j.fuproc.2022.107469.
[14] Mortari DA, Pereira FM, Crnkovic PM. Experimental investigation of the carbon dioxide effect on the devolatilization and combustion of a coal and sugarcane bagasse. Energy 2020;204:117824. https://doi.org/10.1016/j.energy.2020.117824.
[15] Lei K, Ye B, Cao J, Zhang R, Liu D. Combustion characteristics of single particles from bituminous coal and pine sawdust in O_2/N_2, O_2/CO_2 and O_2/H_2O atmospheres. Energies (Basel) 2017;10:1695. https://doi.org/10.3390/en10111695.
[16] Riaza J, Khatami R, Levendis YA, Álvarez L, Gil MV, Pevida C, et al. Combustion of single biomass particles in air and in oxy-fuel conditions. Biomass Bioenergy 2014;64:162–74. https://doi.org/10.1016/j.biombioe.2014.03.018.
[17] Díez LI, García-Mariaca A, Canalís P, Llera E. Oxy-combustion characteristics of torrefied biomass and blends under O_2/N_2, O_2/CO_2 and $O_2/CO_2/H_2O$ atmospheres. Energy 2023;284:128559. https://doi.org/10.1016/j.energy.2023.128559.
[18] Gil MV, Riaza J, Álvarez L, Pevida C, Rubiera F. Biomass devolatilization at high temperature under N_2 and CO_2: Char morphology and reactivity. Energy 2015;91:655–62. https://doi.org/10.1016/j.energy.2015.08.074.
[19] Faúndez J, Arias B, Rubiera F, Arenillas A, García X, Gordon AL, et al. Ignition characteristics of coal blends in an entrained flow furnace. Fuel 2007;86:2076–80. https://doi.org/10.1016/j.fuel.2007.03.024.
[20] Komaki A, Gotou T, Uchida T, Yamada T, Kiga T, Spero C. Operation experiences of oxyfuel power plant in Callide oxyfuel project. Energy Procedia 2014;63:490–6. https://doi.org/10.1016/j.egypro.2014.11.053.
[21] Anheden M, Burchhardt U, Ecke H, Faber R, Jidinger O, Giering R, et al. Overview of operational experience and results from test activities in Vattenfall's 30 MW_{th} oxyfuel pilot plant in Schwarze Pumpe. Energy Procedia 2011;4:941–50. https://doi.org/10.1016/j.egypro.2011.01.140.
[22] Wu H, An Z, Zhang K, Mao Y, Zheng Z, Liu Z. Experimental study on NO_x emission characteristics under oxy-fuel combustion. Clean Energy 2023;7:595–601. https://doi.org/10.1093/CE/ZKAD007.
[23] Wang X, Tan H, Niu Y, Pourkashanian M, Ma L, Chen E, et al. Experimental investigation on biomass co-firing in a 300 MW pulverized coal-fired utility furnace in China. Proceedings of the Combustion Institute 2011;33:2725–33. 10.1016/j.proci.2010.06.055.
[24] Munir S, Nimmo W, Gibbs BM. The effect of air staged, co-combustion of pulverised coal and biomass blends on NOx emissions and combustion efficiency. Fuel 2011;90:126–35. https://doi.org/10.1016/j.fuel.2010.07.052.
[25] Skeen SA, Kumfer BM, Axelbaum RL. Nitric oxide emissions during coal and coal/biomass combustion under air-fired and oxy-fuel conditions. Energy Fuel 2010;24:4144–52. https://doi.org/10.1021/ef100299n.
[26] Wang X, Ren Q, Li W, Li H, Li S, Lu Q. Nitrogenous gas emissions from coal/biomass co-combustion under a high oxygen concentration in a circulating fluidized bed. Energy Fuel 2017;31:3234–42. https://doi.org/10.1021/acs.energyfuels.6b03141.
[27] Liu Q, Zhong W, Yu H, Tang R, Yu A. Experimental studies on the emission of gaseous pollutants in an oxy-fuel fluidized bed with the cofiring of coal and biomass waste fuels. Energy Fuel 2020;34:7373–87. https://doi.org/10.1021/acs.energyfuels.0c01061.
[28] Li W, Liu D, Li S, Kong R. Combustion performance and ash compositions during biomass/semi-coke blended fuel oxy-fuel circulating fluidized bed combustion. Energy Fuel 2020;34:3522–31. https://doi.org/10.1021/acs.energyfuels.9b04323.
[29] Shah IA, Gou X, Zhang Q, Wu J, Wang E, Liu Y. Experimental study on NO_x emission characteristics of oxy-biomass combustion. J Clean Prod 2018;199:400–10. https://doi.org/10.1016/j.jclepro.2018.07.022.
[30] Duan L, Duan Y, Zhao C, Anthony EJ. NO emission during co-firing coal and biomass in an oxy-fuel circulating fluidized bed combustor. Fuel 2015;150:8–13. https://doi.org/10.1016/j.fuel.2015.01.110.
[31] Liu Q, Zhong W, Tang R, Yu H, Gu J, Zhou G, et al. Experimental tests on co-firing coal and biomass waste fuels in a fluidised bed under oxy-fuel combustion. Fuel 2021;286:119312. https://doi.org/10.1016/j.fuel.2020.119312.
[32] Wang Z, Zhou J, Wen Z, Liu J, Cen K. Effect of mineral matter on NO reduction in coal reburning process. Energy Fuel 2007;21:2038–43. https://doi.org/10.1021/ef0604902.
[33] Seepana S, Jayanti S. Steam-moderated oxy-fuel combustion. Energy Convers Manage 2010;51:1981–8. https://doi.org/10.1016/j.enconman.2010.02.031.
[34] Salvador C, Mitrovi M, Zanganeh K. Novel oxy-steam burner for zero-emission power plants. 1st Oxy-fuel Combustion Conference, IEAGHG, Cottbus, Germany, September 2009.
[35] Zou C, Cai L, Wu D, Liu Y, Liu S, Zheng C. Ignition behaviors of pulverized coal particles in O_2/N_2 and O_2/H_2O mixtures in a drop tube furnace using flame monitoring techniques. Proc Combust Inst 2015;35:3629–36. https://doi.org/10.1016/j.proci.2014.06.067.
[36] Zhou H, Li Y, Li N, Cen K. Experimental investigation of ignition and combustion characteristics of single coal and biomass particles in O_2/N_2 and O_2/H_2O. J Energy Inst 2019;92:502–11. https://doi.org/10.1016/j.joei.2018.04.008.
[37] Kops RB, Pereira FM, Rabaçal M, Costa M. Effect of steam on the single particle ignition of solid fuels in a drop tube furnace under air and simulated oxy-fuel conditions. Proc Combust Inst 2019;37:2977–85. https://doi.org/10.1016/j.proci.2018.05.091.
[38] Escudero AI, Aznar M, Díez LI. Oxy-steam combustion: The effect of coal rank and steam concentration on combustion characteristics. Fuel 2021;285:119218. https://doi.org/10.1016/j.fuel.2020.119218.

[39] Deng L, Zhao Y, Sun S, Feng D, Zhang W. Review on thermal conversion characteristics of coal in O_2/H_2O atmosphere. Fuel Process Technol 2022;232:107266. https://doi.org/10.1016/j.fuproc.2022.107266.
[40] Gil MV, Riaza J, Álvarez L, Pevida C, Pis JJ, Rubiera F. A study of oxy-coal combustion with steam addition and biomass blending by thermogravimetric analysis. J Therm Anal Calorim 2012;109:49–55. https://doi.org/10.1007/s10973-011-1342-y.
[41] Lei K, Zhang R, Ye B, Cao J, Liu D. Combustion of single particles from sewage sludge/pine sawdust and sewage sludge/bituminous coal under oxy-fuel conditions with steam addition. Waste Manag 2020;101:1–8. https://doi.org/10.1016/j.wasman.2019.09.034.
[42] Rabaçal M, Kops RB, Pereira FM, Costa M. Direct observations of single particle fragmentation in the early stages of combustion under dry and wet conventional and oxy-fuel conditions. Proc Combust Inst 2019;37:3005–12. https://doi.org/10.1016/j.proci.2018.07.001.
[43] Moroń W, Rybak W. NO_x and SO_2 emissions of coals, biomass and their blends under different oxy-fuel atmospheres. Atmos Environ 2015;116:65–71. https://doi.org/10.1016/j.atmosenv.2015.06.013.
[44] Lu P, Hao J, Yu W, Zhu X, Dai X. Effects of water vapor and Na/K additives on NO reduction through advanced biomass reburning. Fuel 2016;170:60–6. https://doi.org/10.1016/j.fuel.2015.12.037.
[45] Jurado N, Simms NJ, Anthony EJ, Oakey JE. Effect of co-firing coal and biomass blends on the gaseous environments and ash deposition during pilot-scale oxy-combustion trials. Fuel 2017;197:145–58. https://doi.org/10.1016/j.fuel.2017.01.111.
[46] An F, Dai Z, Guhl S, Gräbner M, Richter A. Detailed analysis of the particle residence time distribution in a pressurized drop-tube reactor. AIChE J 2023;69(6):e18026. https://doi.org/10.1002/aic.18026.
[47] Riaza J, Álvarez L, Gil MV, Pevida C, Pis JJ, Rubiera F. Effect of oxy-fuel combustion with steam addition on coal ignition and burnout in an entrained flow reactor. Energy 2011;36:5314–539. https://doi.org/10.1016/j.energy.2011.06.039.
[48] Zhijun S, Su S, Xu J, Xu K, Hu S, Wang Y, et al. Effects of H_2O on NO emission during oxy-coal combustion with wet recycle. Energy Fuel 2017;31:8392–839. https://doi.org/10.1021/acs.energyfuels.7b00897.
[49] Hecht ES, Shaddix CR, Geier M, Molina A, Haynes BS. Effect of CO_2 and steam gasification reactions on the oxy-combustion of pulverized coal char. Combust Flame 2012;159:3437–47. https://doi.org/10.1016/j.combustflame.2012.06.009.
[50] Xu J, Su S, Sun Z, Si N, Qing M, Liu L, et al. Effects of H_2O gasification reaction on the characteristics of chars under oxy-fuel combustion conditions with wet recycle. Energy Fuel 2016;30:9071–909. https://doi.org/10.1021/acs.energyfuels.6b01725.
[51] Escudero AI, Aznar M, Díez LI, Mayoral MC, Andrés JM. From O_2/CO_2 to O_2/H_2O combustion: The effect of large steam addition on anthracite ignition, burnout and NOx formation. Fuel Process Technol 2020;206:106432. https://doi.org/10.1016/j.fuproc.2020.106432.
[52] Lupiáñez C, Díez LI, Romeo LM. Influence of gas-staging on pollutant emissions from fluidized bed oxy-firing. Chem Eng J 2014;256:380–9. https://doi.org/10.1016/j.cej.2014.07.011.
[53] Sher F, Pans MA, Afilaka DT, Sun C, Liu H. Experimental investigation of woody and non-woody biomass combustion in a bubbling fluidized bed combustor focusing on gaseous emissions and temperature profiles. Energy 2017;141:2069–80. https://doi.org/10.1016/j.energy.2017.11.118.
[54] Glarborg P, Miller JA, Ruscic B, Klippenstein SJ. Modeling nitrogen chemistry in combustion. Prog Energy Combust Sci 2018;67:31–68. https://doi.org/10.1016/j.pecs.2018.01.002.
[55] Sher F, Pans MA, Sun C, Snape C, Liu H. Oxy-fuel combustion study of biomass fuels in a 20 kWth fluidized bed combustor. Fuel 2018;215:778–86. https://doi.org/10.1016/j.fuel.2017.11.039.
[56] Kosowska M, Luckos A, Kijo-Kleczkowska A. Pollutant emissions during oxy-fuel combustion of biomass in a bench scale CFB combustor. Energies (Basel) 2022;15:1–23. https://doi.org/10.3390/en15030706.
[57] Schafer S, Bonn B. Hydrolysis of HCN as an important step in nitrogen oxide formation in fluidised combustion, Part 1: homogeneous reactions. Fuel 2000;79:1239–46. https://doi.org/10.1016/S0016-2361(99)00254-9.
[58] Ndibe C, Spörl R, Maier J, Scheffknecht G. Experimental study of NO and NO_2 formation in a PF oxy-fuel firing system. Fuel 2013;107:749–56. https://doi.org/10.1016/j.fuel.2013.01.055.
[59] Álvarez L, Riaza J, Gil MV, Pevida C, Pis JJ, Rubiera F. NO emissions in oxy-coal combustion with the addition of steam in an entrained flow reactor. Greenhouse Gases Science Technology 2011;1:180–90. https://doi.org/10.1002/ghg.16.
[60] Aarna I, Suuberg EM. A review of the kinetics of the nitric oxide-carbon reaction. Fuel 1997;76:475–91. https://doi.org/10.1016/S0016-2361(96)00212-8.
[61] Arenillas A, Rubiera F, Pis JJ. Nitric oxide reduction in coal combustion: Role of char surface complexes in heterogeneous reactions. Environ Sci Tech 2002;36:5498–503. https://doi.org/10.1021/es0208198.